

# A DYNAMIC MODEL OF ONCE-THROUGH STEAM GENERATOR (OTSG) FOR PROTOTYPICAL ADVANCED REACTOR

**Fan Zhang and Jamie Coble\***  
Department of Nuclear Engineering  
University of Tennessee  
Knoxville, TN 37996 USA  
fzhang17@vols.utk.edu; jamie@utk.edu\*

## ABSTRACT

A new design of Small Modular Reactor, the Prototypical Advanced Reactor (PAR), features two sodium primary systems each connected to dedicated steam generators (SGs) and sharing a balance of plant (BOP) system. PAR adopts once-through steam generators (OTSG) for its compact structure. The existence of superheated steam in a OTSG improves turbine design by eliminating the need of bulky moisture separator in SG. The two cores and SGs' design enable PAR to adjust power flexibly, as a result, introduce more challenges to the control. Therefore, a fast simulation model with high accuracy OTSG model is needed. In this paper, a dynamic model is built for OTSG of PAR based on the conservation of mass, momentum, and energy. The OTSG is simulated as lumped pipe and divided into subcooled, evaporating, and superheated regions by moving boundaries. SIMULINK is adopted to this OTSG simulation to be merged into existing PAR system models easily. The steady state results show that key parameters are rational. The 5% step increase of feedwater enthalpy transient demonstrates that the model is capable to respond to the perturbations. Since the basic laws and algebraic method used in this paper are suitable for other fluids, the model can be easily applied to any other OTSG. Future work will also focus on model optimization, merging and improved control. The final aim is to perform full scope real-time simulations for PAR under normal operational transients.

*Key Words:* OTSG, dynamic model, PAR, SIMULINK

## 1 INTRODUCTION

Small modular reactors (SMRs) are nuclear reactors with less power (300 MWe or less) than traditional full scale plants. The compact designs and factory fabricated features enable them to be transported by truck or rail to a nuclear power site, and used in parallel to get larger total power output. SMRs are planned to be operating commercially within next two decades, and will play a significant role in addressing energy, security, economic, and climate goals. One SMR design, the Prototypical Advanced Reactor (PAR), is a liquid sodium fast breeder reactor design with a power of 40 MWe. There are three loops in PAR: primary loop, intermediate sodium coolant loop, and the secondary loop. As shown in figure 1, Prototypical Advanced Reactor (PAR) includes two independent reactor cores [1], each connected to a dedicated intermediate Heat eXchanger (HX) and Steam Generator (SG). Steam from the two modules mixes within one steam header, and is sent to the common balance of plant (BOP) system to generate electricity.

PAR adopts Once-through steam generator (OTSG) for its configuration is compact enough to enable it to be located in the pressure vessel. The existence of superheated steam in OTSG eliminates the bulky moisture separator in SG and benefits for turbines. Those advantages make OTSGs are widely used in SMRs' design.

---

\* Corresponding author: Jamie Coble

The SG is one of the most important components in nuclear power plants, which always need special attention. The dual-SG design in PAR introduces extra challenges for control than the traditional one SG design, especially under the situations that the two reactor cores in PAR operate at different power levels. The steam from a SG is an important variable in nuclear plant control, which is both needed in BOP system control and reactor power control. Therefore, a good OTSG model is needed for whole system simulation.

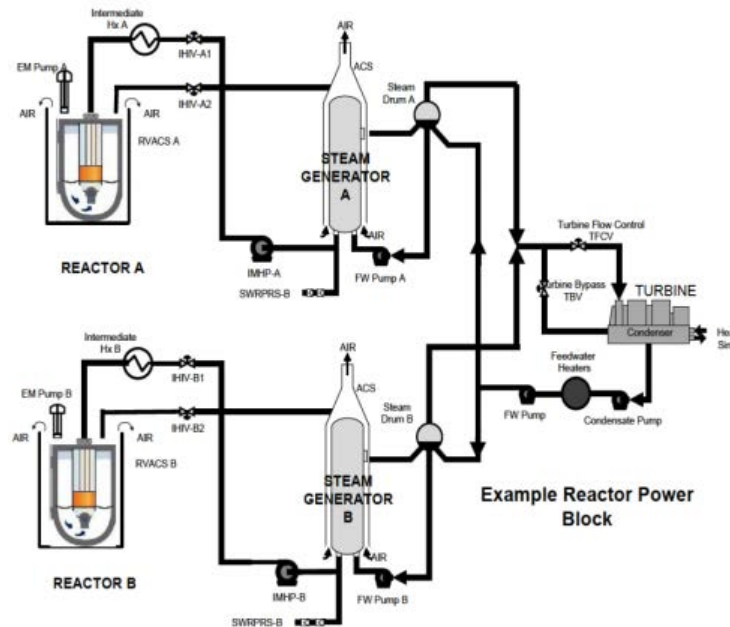


Figure 1. Prototypical advanced reactor power blocks [1]

Before building a new type of nuclear system, simulations are used to assess the performance and the consequences of possible configuration changes to provide information and instruction. Two kinds of dynamic models are widely used for single device in nuclear system such as steam generators. One is fine mesh model, which typically involves the distributed parameter described by partial differential equations and its discretization equations. It is mainly used for detailed thermal hydraulic analysis and has high accuracy which need much calculation time [2]. The other model is the lumped parameter model described by ordinary differential equations (ODEs), which is mainly used for fast simulation, compound system simulation and control system encompassed simulation. For this kind of simulation, the models should be high fidelity and faster than the former kind, which is able to simulate the perturbation responses of the nuclear power plant fast. This kind of model is suitable to assess the full scope compound system performance and train operators. In addition, it can be used to define relationships between a set of plant signals, which is useful for equipment health monitoring, diagnostics, and prognostics. A SIMULINK model of the PAR system of was previously developed [3]. This model used a linearized perturbation model of the SG; to improve the performance of whole system model, a dynamic nonlinear model for OTSG of PAR is built in this paper, which will be integrated in the full PAR model in the future.

Previous research has been completed for OTSG simulation. Li et al. has developed a lumped parameter model of the helical coiled OTSG of the 10 MW high-temperature gas-cooled reactor (HTR-10) [4]. Dong has developed a model for the OTSG of modular high temperature gas-cooled reactor (MHTGR), which has been applied to the real-time simulation software for the operation and regulation features of MHTGR-based commercial nuclear plant [5]. The fluid in primary side of OTSG in the research of both Li and Dong is helium. Zhu et al. has developed a dynamic model for OTSG with

concentric annuli tube using Gear method. The fluid in primary side is water [6]. Berry developed a model of OTSG with sodium as the primary fluid, however, the method is not convenient to be modeled by SIMULINK [7]. Therefore, a dynamic model for OTSG with sodium as primary fluid is developed in this paper.

All of these researches apply moving boundary method into OTSG simulation. Since moving boundary method describes the heat transfer character appropriately, it also be adopted in this paper. Based on conservation laws of mass, momentum, and energy, this paper gives the algebraic model for OTSG with sodium in the primary side. Two moving boundaries divide OTSG into subcooled region, evaporating region and superheated region. Steady state for the OTSG model is conducted by SIMULINK, which shows that the steady-state calculation results are rational. The transient of 5% step increase of feedwater enthalpy is conducted and results show the key parameters changes are rational and reach the new steady state. Future work will focus on the model optimizing, model merging and controller improving. The real-time full-scope simulation and control for PAR under operational steady state and transient will be achieved in the future.

## 2 METHODOLOGY

The dynamic model for OTSG is developed in this part. Figure 2 shows the flow chart of method solution. The OTSG model involves solving conservation equations for both primary side and secondary side, tube wall equations, fluids properties calculation and heat transfer models. The details of these blocks are described in this section.

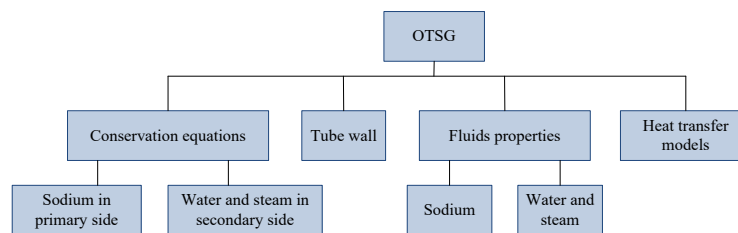
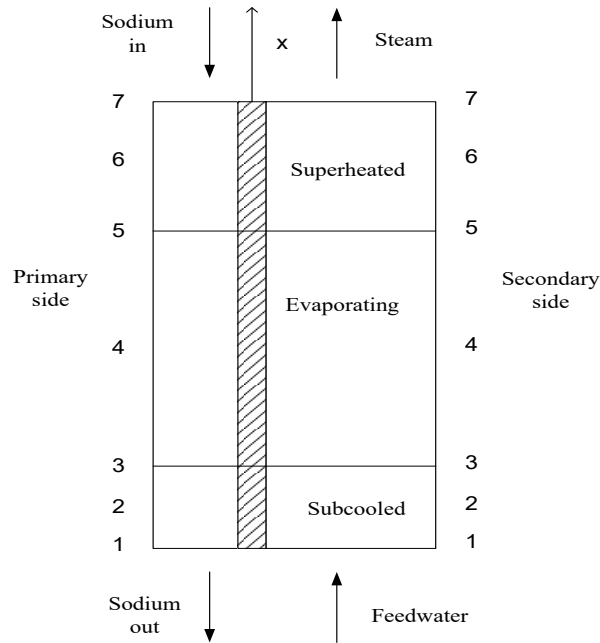


Figure 2. the flow chart of method solution

### 2.1 Description of OTSG Nodes in PAR and Assumptions

The OTSG of PAR is a vertical, shell-and-tube type SG. The counter flow design is used to obtain effective heat transfer between two sides of OTSG. Fluid in the primary side of OTSG is the single-phase sodium, which is the sodium in intermediate coolant loop of PAR. The fluids in the secondary side are water and steam, which are in secondary loop of PAR. To model the OTSG performance better, the OTSG fluid channel are divided into three regions, which are subcooled region, evaporating region, and superheated region, with two moving boundaries, which are defined according to the specific enthalpy of water in the secondary side. Subcooled region is the region where the fluid enthalpy is less than saturated water enthalpy; nucleate boiling region is the region where the fluid enthalpy is equal to or greater than saturated water enthalpy but less than saturated steam enthalpy; the superheated region is the region where the fluid enthalpy is greater than saturated steam enthalpy. In this paper, two phase flow in all the tubes of the OTSG are assumed to be homogenous, which is a common assumption in fast fluid modeling [4][5][6]. Therefore, both sides of OTSG are lumped and treated as single straight flow channel.



**Figure 3. Nodes scheme of OTSG model**

Figure 3 shows the nodal scheme of OTSG model. Point 1 to 3 is the subcooled region and point 2 is the central point of this region. Point 3 to 5 is the evaporating region and point 4 is the central point of this region. Point 5 to 7 is the superheated region and point 6 is the central point of this region. Since the boundaries between regions are movable, so the length of subcooled region  $L_{13}$  and length of superheated region  $L_{15}$  vary by time, which are set as state variables. The nodes in primary side are the same with the secondary side for easy calculation.

Since the SIMULINK model in this paper is for future whole PAR system model simulation to facilitate perturbation assessment, health monitoring, diagnostics and prognostics, the calculation speed is an important evaluation. To enable model high speed while little sacrifices of accuracy, two reasonable assumptions are made: Axial heat conduction is ignored; Enthalpy and pressure in the same heat transfer region varies linearly, which means these values of central point can be calculated by the nearby boundary points.

## 2.2 Conservation Equations and Algebraic Method

Sodium in primary side, water and steam in secondary side all follow the conservation laws of mass momentum and energy describes by Equation (1) (2) (3) with the coordinate frame given in figure 3.

$$\frac{\partial \rho}{\partial t} = -\frac{\partial(\rho u)}{\partial x} \quad (1)$$

$$\frac{\partial(\rho u)}{\partial t} = -\frac{\partial(\rho u^2)}{\partial x} - \frac{\partial P}{\partial x} - \frac{\rho u^2}{2} \frac{F_f S}{A} - \rho g \quad (2)$$

$$\frac{\partial(\rho h)}{\partial t} = -\frac{\partial(\rho hu)}{\partial x} + \frac{q}{A} + \frac{\partial P}{\partial t} \quad (3)$$

where  $\rho$  is the fluid density (kg/m<sup>3</sup>),  $u$  is the fluid velocity (m/s),  $P$  is the fluid pressure (Pa),  $F_f$  is the friction factor,  $S$  is the wetted perimeter (m),  $A$  is cross sectional area (m<sup>2</sup>),  $g$  is the gravitational acceleration (N·m/s<sup>2</sup>),  $h$  is the fluid specific enthalpy (J/kg), and  $q$  is the heat flux per unit length (W/m<sup>2</sup>).

Apply equation (1)(2) (3) for both primary side and secondary side for the OTSG based on the nodes in Figure 2. By integrating the mass conservation equation and energy conservation equation in different regions respectively along x-axis direction using the Leibniz theorem [8], the ODEs can be obtained. For example, equation (4) and (5) shows the ODEs for fluid in secondary side in subcooled region.

$$\frac{d(\rho_{s2}l_{13})}{dt} - \rho_{s2} \frac{dl_{13}}{dt} + D_{s3} - D_{s1} = 0 \quad (4)$$

$$\frac{d(h_{s2}\rho_{s2}l_{13})}{dt} - \rho_{s3}h_{s3} \frac{dl_{13}}{\partial t} + D_{s3}h_{s3} - D_{s1}h_{s1} = \frac{Q_2}{A_{s2}} + \frac{dp_{s2}l_{13}}{dt} - p_{s3} \frac{dl_{13}}{dt} \quad (5)$$

where  $l_{13}$  is the length of subcooled region (m),  $D$  is the fluid mass velocity (kg/(s·m<sup>2</sup>)), and  $Q_2$  is the heat flux in the subcooled region (W). The explanation of subscripts is shown in Table 1.

**Table I. Explanation of subscription**

Subscription	s	m	fw	1,2,3,4,5,6,7
Explanation	Secondary side	Metal tube wall	Feedwater	Point 1,2,3,4,5,6,7

The enthalpy in node 2 is equal to the average of enthalpy in node 1 and 3. Since the fluid in node 3 is saturated, the enthalpy is just the function of pressure. So equation (5) can be described as equation (6).

$$\left[ \frac{\rho_{s3}(h_{s1} - h_{s3})}{2} + (P_{s3} - P_{s1}) \right] \frac{dl_{13}}{dt} + \frac{\rho_{s3}l_{13}}{2} \frac{dh_{s1}}{dt} = \frac{l_{13}}{2} \left( 1 - \rho_{s2} \frac{\partial h_{s3}}{\partial P_{s3}} (P = P_{s3}) \right) \frac{dP_{s3}}{dt} + (G_{s1}/A_{s1} + G_{s3}/A_{s3})(h_{s1} - h_{s3})/2 + \frac{Q_2}{A_{s2}} \quad (6)$$

Taking time-delay of secondary inlet the subcooled region into consideration, the fluid flow rate in node 3 and the enthalpy in node 1 can be presented by first-order delay as shown in equation (7) and (8) [8].

$$\frac{dh_{s1}}{dt} = \frac{h_{fw} - h_{s1}}{\tau_s} \quad (7)$$

$$\frac{dG_{s3}}{dt} = \frac{G_{s1} - G_{s3}}{\tau_s} \quad (8)$$

Since the pressure-flow process dynamic behavior is much faster than the enthalpy-temperature dynamic behavior, the time-dependent term in the momentum equation can be ignored to simplify the equation (2) as shown below [4].

$$\frac{\partial(\rho u^2)}{\partial x} + \frac{\partial P}{\partial x} = -\frac{\rho u^2}{2} \frac{F_f S}{A} - \rho g \quad (9)$$

Integrate equation 6 in the subcooled region, we can get the following equation:

$$P_{s3} - P_{s1} = -\rho_{s2} g l_{13} - F_{fs2} l_{13} D_{s2}^2 \quad (10)$$

Derive equation (10) to obtain equation (11)

$$\frac{dP_{s3}}{dt} = -(\rho_{s2} g + F_{fs2} G_{s2}^2 / A_{s2}^2) \frac{dl_{13}}{dt} - \frac{F_{fs2} G_{s3}}{A_{s2}^2} \frac{dG_{s3}}{dt} \quad (11)$$

The mass flow of point 3 to point 7 are treated as equal since the density in these two regions are much less than in the subcooled region. Applying the same method for evaporating region and superheated region to get the ODEs.

### 2.3 Equations for Tube Wall

General heat conduction equation is

$$\rho c \frac{dT}{dt} = \phi \quad (12)$$

where  $\rho$  is the density (kg/m<sup>3</sup>),  $c$  is the specific heat (J/kg\*K),  $T$  is the temperature (K),  $\phi$  is the heat production per volume (W/m<sup>3</sup>)

Integrate equation (12) using Leibnitz theorem in each region of tube wall, we can obtain equations (13) (14) and (15).

$$\frac{dT_{m2}}{dt} = \frac{Q_{m2}}{A_{m2} \rho_{m2} c_{m2} l_{13}} + \frac{T_{m4} - T_{m2}}{l_{15}} \frac{dl_{13}}{dt} \quad (13)$$

$$\frac{dT_{m4}}{dt} = \frac{Q_{m4}}{A_{m4} \rho_{m4} c_{m4} (l_{15} - l_{13})} + \frac{T_{m6} - T_{m4}}{l_{17} - l_{13}} \frac{dl_{15}}{dt} + \frac{T_{m4} - T_{m2}}{l_{15}} \frac{dl_{13}}{dt} \quad (14)$$

$$\frac{dT_{m6}}{dt} = \frac{Q_{m6}}{A_{m6} \rho_{m6} c_{m6} (l_{17} - l_{15})} + \frac{T_{m6} - T_{m4}}{l_{17} - l_{13}} \frac{dl_{15}}{dt} \quad (15)$$

### 2.4 Heat Transfer Models

Convection heat transfer between primary and secondary side is convection heat transfer. The general heat flux of convection heat transfer is given by equation (16).

$$q = h_t (T_1 - T_2) \quad (16)$$

where  $q$  is the heat flux,  $h_t$  is the heat transfer coefficient,  $T_1$  is the temperature of subject 1, and  $T_2$  is the temperature of subject 2.

The heat transfer model is described by nine equations: convection heat transfer equations between sodium in primary side and tube wall surface in primary side in three regions; conductivity heat transfer equations within tube wall in different regions; convection heat transfer equations between tube wall

surface in secondary side and fluid in secondary side in different regions. The heat transfer coefficient used for sodium in primary side to metal tube wall is 7046.77 W/m<sup>2</sup>\*K according to Reference [9].

The fluid status in the secondary side of OTSG are different. The Dittuse-Bolter correlation is used for single-phase liquid in subcooled region and single-phase steam in superheat region [10].

$$Nu = 0.023 Re^{0.8} Pr^{0.33} \quad (17)$$

where Re and Pr is the Reynolds number and the Prandtl number of fluid, respectively.

Chen correlation is used in evaporating region [11]. In Chen correlation, two basic mechanisms in the heat transfer process for the fluid flow boiling are taken in to consideration. They are the ordinary macro-convective mechanism of heat transfer in flowing fluids, and the micro-convective mechanism related to bubble-nucleation and growth. So the total heat transfer is contributed by these two mechanisms additively as equation (18).

$$h = h_{mic} + h_{mac} \quad (18)$$

where the h is total heat transfer coefficient, h<sub>mic</sub> is the micro convective mechanism heat transfer coefficient, and h<sub>mac</sub> is the macro convective mechanism heat transfer coefficient. Forster and Zuber's formulation is used to calculate h<sub>mic</sub> [11].

$$h_{mic} = 0.00122 \left[ \frac{\lambda_f^{0.79} c_{p,f}^{0.45} \rho_f^{0.49} G^{0.23}}{\sigma^{0.5} \mu_f^{0.29} h_{fg}^{0.24} \rho_g^{0.24}} \right] \Delta T^{0.24} \Delta P^{0.75} Su \quad (19)$$

where  $\lambda$  is the thermal conductivity (Btu/h\*ft\* °F),  $C_p$  is the heat capacity (Btu/lb\*°F),  $G$  is the gravitational constant,  $\sigma$  is the vapor-liquid surface tension (lb/ft),  $h_{fg}$  is the latent heat of vaporization (Btu/lb),  $\Delta T$  is the wall superheat (°R), and  $\Delta P$  is the pressure difference corresponding to the wall superheat (psf).  $Su$  is the suppression factor represents the ratio of the effective superheat to the total superheat of the wall, subscript f stands for liquid water phase and g for steam phase.

The macro convective heat transfer coefficient h<sub>mac</sub> is calculated by

$$h_{mac} = 0.023 Re_f^{0.8} Pr_f^{0.4} \frac{\lambda_f}{D} F \quad (20)$$

where D is the hydraulic diameter (m) and F is the ratio of the two-phase Reynolds number to the liquid Reynolds number, which is calculated by Martinelli parameter  $X_{tt}$  [11].

## 2.5 Fluids Properties Calculation

The sodium in primary side is the single-phase sodium. Therefore, the sodium properties involved in this model uses lumped parameter from two references [9][12].

Lots of properties of water and steam are involved in this model state, including density, enthalpy, heat conductivity coefficient, viscosity, surface tension, specific heat, latent heat, saturated pressure based on temperature. After compared international water and steam calculation formulations [13], "International Association for the Properties of Water and Steam Industrial Formulation 1997" (IAPWS-IF97) is adopted in this model to calculate the properties of water and steam [14].

## 2.6 Inputs of SIMULINK Model

To solve the equations above, select primary sodium pressure, enthalpy, mass flow at the inlet point and secondary feedwater pressure, enthalpy, mass flow at the inlet point as six input variables, which can be provided by PAR IHX and BOP system calculation when merged into the PAR whole system simulation.

## 3 RESULTS AND DISCUSSION

The steady-state simulation was performed and all the key parameters can reach to the steady. The calculation results show that subcooled region length is 10.82m and the evaporation region length is 20.78m. Figure 4 shows the 500s steady state simulation of temperature in different regions of the two sides of metal wall between the primary and secondary side of OTSG and the enthalpy of deferent regions of the primary sodium and the water and steam in the secondary side. The surface temperature of metal wall in primary side is higher than the surface temperature of metal wall in secondary side. The values of these key parameters are rational to the OTSG design.

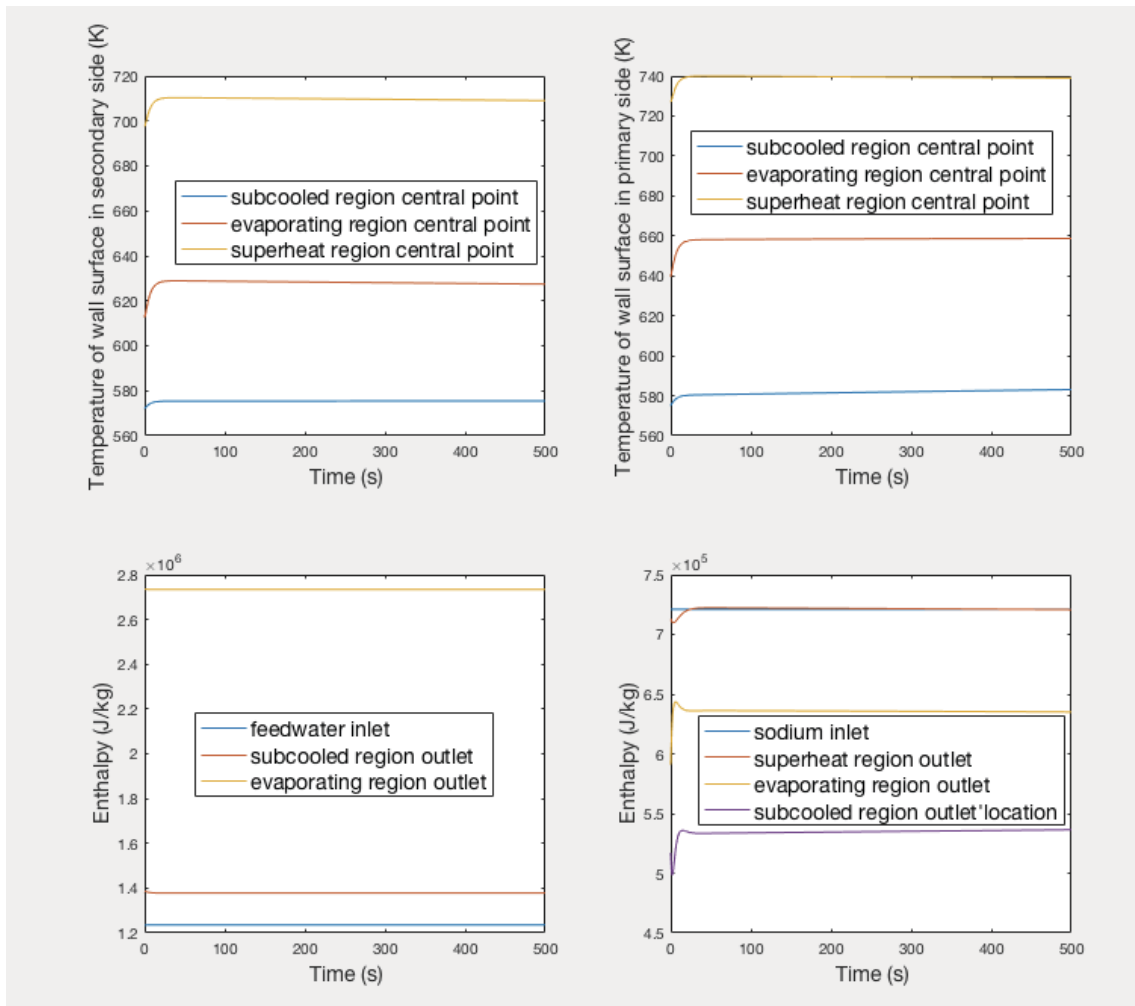
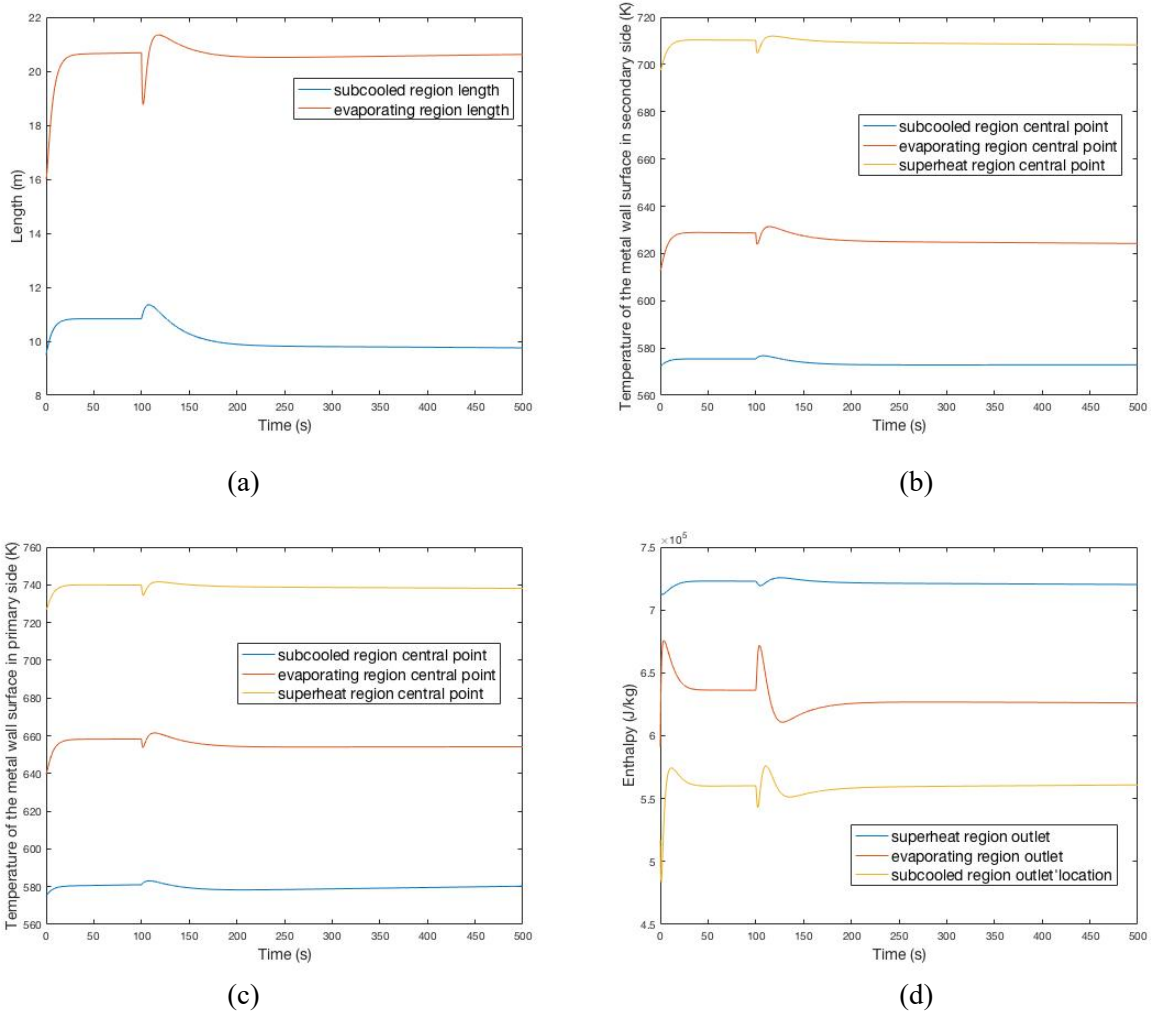


Figure 4. Steady state of key parameters



The 5% increase of the feedwater enthalpy transient is conducted. At first, the system is performing the steady state 100s without any perturbation and a 5% feedwater enthalpy step increase is insert at 100s. Figure 5(a) shows the subcooled region length and evaporation region length in 5% step increase of feedwater enthalpy transient. The subcooled region decreases with the enthalpy increases because that the heat needed for preheating the feedwater to saturated water decreases. Figure 5(b) shows the surface temperature in different regions of the metal wall in secondary side. Figure 5(c) shows the surface temperature in different regions of the metal wall in primary side. Figure 5(d) shows sodium enthalpy in different regions. The parameters in figure 5(b-d) decrease slightly after the 5% step increase of feedwater enthalpy perturbation, because the increased feedwater enthalpy makes heat transfer between the OTSG primary side and secondary side decrease. Figure 5 shows that the parameters can reach new steady state. The key parameters changes in transient are rational.



**Figure 5. Response to a 5% step increase of feedwater enthalpy transient in the (a) subcooled region length and evaporation region length, (b) surface temperature in different regions of the metal wall in secondary side, (c) surface temperature in different regions of the metal wall in primary side, and (d) Sodium enthalpy in different regions**

## 4 CONCLUSIONS

A dynamic model of OTSG for PAR is developed in this paper. The OTSG is divided into subcooled, evaporating and superheated region by two moving boundaries according to the enthalpy of the secondary fluid. The model is based on the conservation laws of mass, momentum, and energy, and solved by integrating using Leibnitz theorem. For heat transfer models, Chen correlation is used in evaporating region and the Dittuse-Bolter correlation is used for both single-phase liquid in subcooled region and single-phase steam in superheat region. IAPWS-IF97 is used for the properties of water and steam calculated for its high accuracy.

Simulation of the OTSG model is carried out by SIMULINK, which is easy to be merged into the existing PAR system model and has good graphic function. The steady-state results show that OTSG model can reach steady-state and the results are rational. The 5% step increase of feedwater enthalpy perturbation transients is conducted to demonstrate that the model is able to respond to perturbation and build new steady state. More transient analysis will be done before the next stage of model optimizing, merging and control improving. The high-performance real-time full-scope simulation for PAR will be developed in the future.

## 5 REFERENCES

1. Coble, J.B., et al., "Technical Needs for Enhancing Risk Monitors with Equipment Condition Assessment for Advanced Small Modular Reactors," PNNL-22377, SMR/ICHMI/PNNL/TR-2013/02, Pacific Northwest National Laboratory, Richland & USA (2013).
2. Daogang Lu, Yu Wang, Bo Yuan, Danting Sui, Fan Zhang et al., "Development of three-dimensional thermal-hydraulic analysis code for steam generator with two-fluid model and porous media approach," *Applied Thermal Engineering*, **Vol. 116**, pp. 663-676 (2017).
3. Xiaotong Liu, "Modeling and Simulation of a Prototypical Advanced Reactor," *M.S. thesis*, Department of Nuclear Engineering., The University of Tennessee, Knoxville & USA (2016).
4. Li, Haipeng, Huang, Xiaojin, Zhang, Liangju, "A lumped parameter dynamic model of the helical coiled once-through steam generator with movable boundaries," *Nuclear Engineering and Design*, **Vol. 238**, pp.1657-1663 (2008).
5. Zhe Dong, "A Differential-Algebraic Model for the Once-Through Steam Generator of MHTGR-Based Multimodular Nuclear Plants," *Mathematical Problems in Engineering*, **Vol. 2015**, 12 pages (2015).
6. Zhu Jingyan, Guo Yun, Zhang Zhijian, "Dynamic simulation of once-through steam generator with concentric annuli tube," *Annals of Nuclear Energy*, **Vol. 238**, pp.1657-1663 (2008).
7. Greg Berry, "Model Of a Once-Through Steam Generator With Moving Boundaries and a Variable Number Of Nodes," *ASME Winter Annual Meeting*, Boston, MA, USA (1983).
8. Leibniz, "Supplementum Geometriae Dimensoriae, Seu Generalissima Omnium Tetragonismorum Effectio Permotum: Similiterque Multiplex Constructio Lineae ex Data Tangentium conditione," *Acta Eruditorum*, pp. 385–392 (1693).
9. Berkan, R.C. and B.R. Upadhyaya, "Dynamic Modeling of EBR-II for Simulation and Control," *Annual Report*, The University of Tennessee, Knoxville & USA (1988).
10. Dittus FW, Boelter LMK, "Heat Transfer in Automobile Radiators of the Tubular Type," *International Communications in Heat and Mass Transfer*, **Vol. 12**, pp. 3-22 (1985).

11. Chen JC, "A Correlation for Boiling Heat Transfer to Saturated Fluids in Convective Flow," *Process Design and Development*, **Vol. 5**, pp. 322-327 (1966).
12. Zengyuan Qian, *Thermal Physical Properties of Metal with Low Melting Point*, Science Press., Shuang Fu & China (1983).
13. Fan Zhang, Dao-gang Lu, Dan-ting Sui, Bo Yuan, and Chao Guo, "Preliminary Development of Thermal Power Calculation Code H-Power for a Supercritical Water Reactor," *Science and Technology of Nuclear Installations*, **Vol. 2014**, 10 pages (2014).
14. Cooper JR, *Revised Release on the IAPWS Industrial Formulation 1997 for the Thermodynamic Properties of Water and Steam*, International Association for the Properties of Water and Steam, Lucerne & Switzerland (2007).